

EVALUATION OF STRENGTH OF SOILS AGAINST LIQUEFACTION USING PIEZO DRIVE CONE

Shun-ichi Sawada¹

ABSTRACT

This paper presents the results obtained from a series of in-situ tests using “*Piezo Drive Cone*” which is dynamic penetrometer with pore pressure transducer (the name is “*DPTU*”). The excess pore pressures generated at the tip of cone during dynamic penetration into ground were measured. It clearly shows from our experiments that, in shallower than the groundwater table, the maximum excess pore pressures just after the blow were generated up to significant pressure, while, in deeper than the groundwater table, these were not observed. The maximum excess pore pressure ratio ($\Delta u_{\max}/\sigma_v$) which is normalized the total overburden stress (σ_v) were good discriminations of the groundwater table. On the other hand, the residual cumulative pore pressure ratio (u_R/σ'_v) at the finishing the penetration phase after blows indicate the classification and identification of soils. Finally, we are immediately able to evaluate the strength of soils against liquefaction using only in-situ data.

Keywords: In-situ test, Liquefaction, Pore pressure, Cone penetration test

INTRODUCTION

It is clear that the evaluation of strength of soils against liquefaction is increasingly important to forecast the damage of structures under the earthquake. N value in the standard penetration test (*SPT*) and the grain size distribution in laboratory test result obtained are both necessary for even simple estimation of the liquefaction susceptibility in the current design specification. Furthermore, in order to estimate the liquefaction susceptibility in detail, cyclic undrained triaxial test using the undisturbed sample has been executed. It follows that these ordinarily investigations have to take a long response time and too expensive to get result. Moreover, in most cases, it becomes difficult to reach to the exact data under a wide area of un-uniformed ground conditions in spite of estimating liquefaction susceptibility specifically from the limited locations. Hence, more simple method which can estimate in-situ liquefaction susceptibility quickly is required to be suggested. This paper will introduce the new method of estimating liquefaction susceptibility using new developing system of dynamic penetrometer with pore pressure transducer named “*Piezo Drive Cone*”; the nation is “*DPTU*”¹⁾⁻⁷⁾.

ESTIMATING LIQUEFACTION SUSCEPTIBILITY IN SEISMIC DESIGN SPECIFICATION

Nowadays the method we use to estimate liquefaction susceptibility adopted in current seismic design specifications and standards⁸⁾⁻¹¹⁾ are based on either F_L method or limited N value method. These methods are all based on N value from the standard penetration test (*SPT*) which is one of the in-situ dynamic penetration tests. These methods have to be used to estimate liquefaction susceptibility by using not only N value and groundwater table (*GWT*) but also unit weight (γ) and fine fraction content (F_C).

¹ Earthquake Geotechnical Engineering Group, OYO Corporation, Tsukuba, Japan, Email: sawada-shun@oyonet.oyo.co.jp

EQUIPMENT AND PROCEDURES OF “PIEZO DRIVE CONE”

Developed dynamic penetrometer with pore pressure transducer *DPTU* is a new investigation tool that measures the pore pressure of the ground which generated during dynamic penetration at the cone tip. Figure 1 shows the schematic figure of general *DPTU* system. This system consists of cone tip with pore pressure transducer, penetration displacement sensor, trigger, data logger and dynamic penetration equipment.

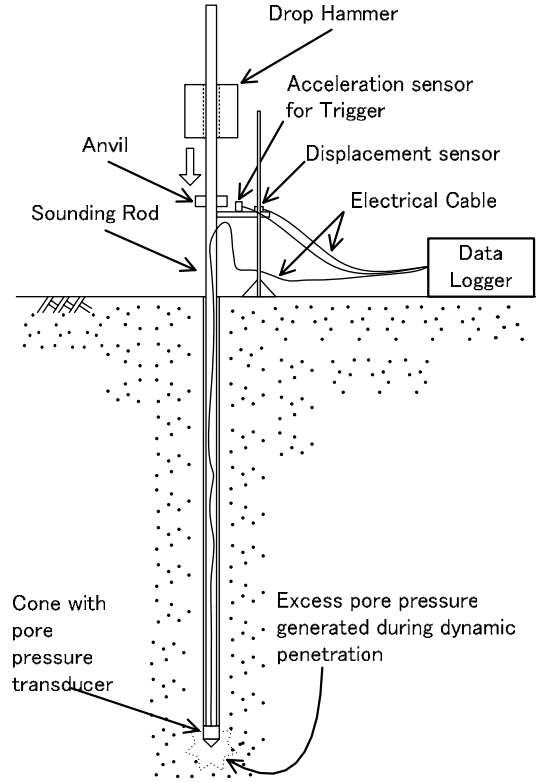


Figure 1. Schematic figure of *DPTU*

In this examination, we used the light weight dynamic penetration device modified the Swedish Ram Sounding test equipment (*Mini Ram*)¹²⁾. The view of *Mini Ram* equipment is shown in Figure 2. However, *DPTU* should not be limited for any particular dynamic penetration equipment. The view of the *DPTU* cone apex is shown in Figure 3. And the cross section of *DPTU* cone tip is also drawn in Figure 4. This light weight dynamic penetration equipment is driven down mechanically by a 30 kg drop hammer with a height of 35 cm free fall. The penetration resistance is taken as the number of blow counts (N_m) required to drive the penetrometer 20 cm downwards. The new defined blow counts N_d values are equal to a half of *Mini Ram* N_m values. And N_d values are nearly equal to these SPT N values (N_{SPT}) as follows,

$$N_{SPT} \approx N_d = 1/2 N_m \quad (1)$$

This relation holds good in a range of the soft ground which liquefaction occurs.

Sounding rods are 28 mm in diameter, with a cylindrical point of *DPTU* cone 36.6 mm in diameter, 69 mm in length and 90 degree in apex angle. External diameter of the cone apex and the rod diameter are designed in different size to reduce frictional force resistance. The porous stones which are measuring pore pressure are located at the cone apex as clearly shown in Figure 3. The data logger records the penetration displacement and the pore pressure response of every blow at the cone apex. The dynamic pore pressure signals are transmitted via an electrical cable pre-threaded down the hollow sounding rods. This data acquisition system includes analogue to digital converters, so that the analogue signals can be immediately converted to digital forms, allowing real-time inspection of the test results in this data acquisition system.

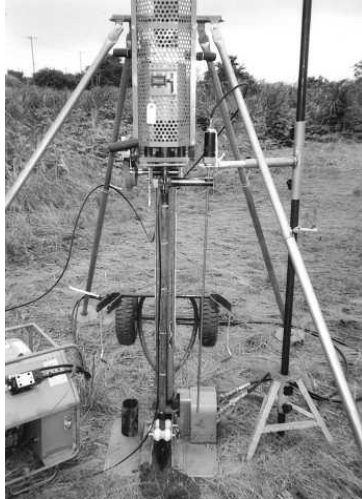


Figure 2. Mini-Ram



Figure 3. cone apex

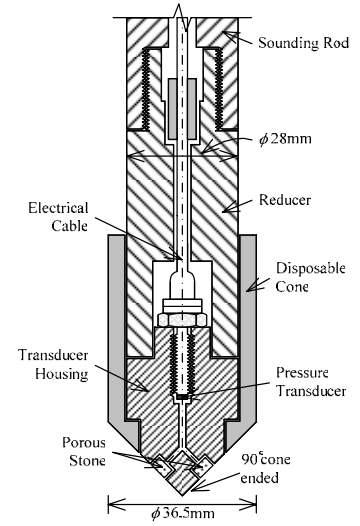


Figure 4. Cross section of cone

IN-SITU TEST RESULT

Evaluation of dynamic penetration resistance

In order to have a continuous profile of the penetration resistance, from the penetration length measured for each blow an equivalent N_d value have been computed. It clearly shows in figure 5 that *Mini Ram* N_d values well coincide with N_{SPT} values which executed in close vicinity to the *DPTU* location and the continuity of N_d value indicates significant change by inter-bedded thin layers. It cannot reasonably be assumed that N_{SPT} values at interval of 1m can classify these thin layers and alternate layer condition.

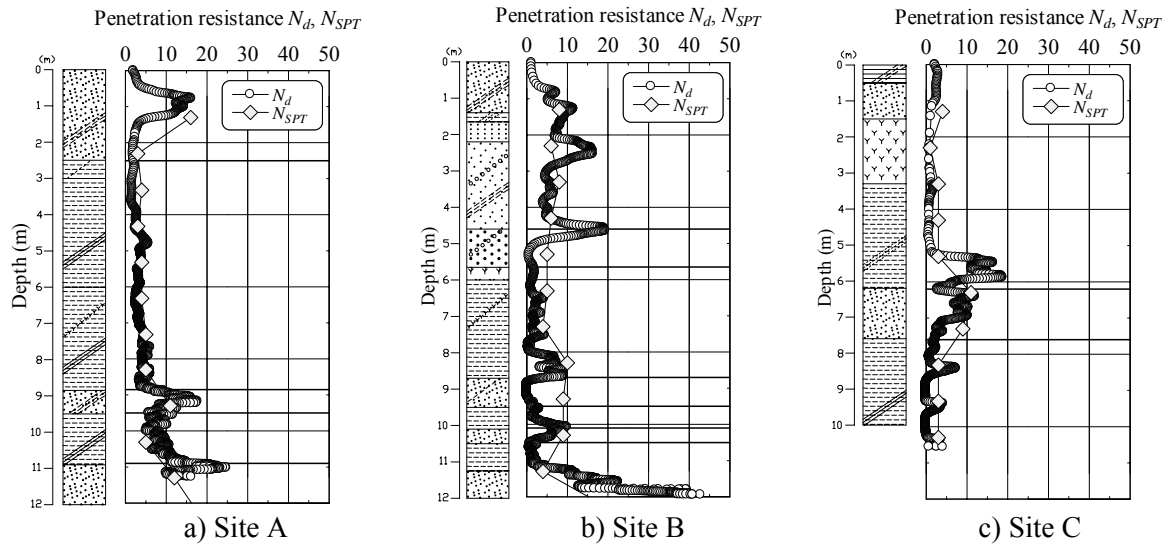


Figure 5. Depth distribution of penetration resistance N_d and N_{SPT}

Evaluation of groundwater table (GWT)

In the *DPTU*, the trigger locks automatically when hammer drops on the anvil. After blows, the time responses of pore pressure and penetration displacement are immediately recorded at high speed ($\Delta t=100\mu\text{sec}$) in the data acquisition component. Typical time histories of penetrated displacement and excess pore pressure ratios are shown in Figure 6. In order to evaluate groundwater table (GWT), the most focused part of this time histories is that the maximum excess pore pressure (Δu_{\max}) during dynamic penetration. One significant response of the excess pore pressure is that drop hammer makes inertia force upward pressure receiving the diaphragm of pressure transducer. Apparent maximum excess pore pressure affected by this inertia force rapidly changes at groundwater table due to the

coefficient of volume compressibility in the ground. In deeper than groundwater table, maximum excess pore pressures (Δu_{\max}) are small because the volume compressibility of the ground restrain the diaphragm modification. On the other hand, in shallower level, they are large because the volume compressibility of the ground does not restrain which is caused by the air existence in the ground. We introduce new method of estimating groundwater table by using these apparent Δu_{\max} .

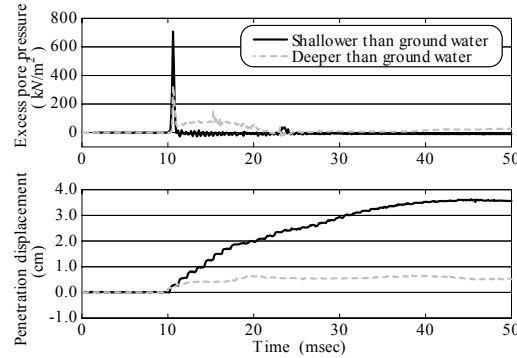


Figure 6. Example of measurement record

Figure 7 shows the distribution of maximum excess pore pressure ratio ($\Delta u_{\max}/\sigma_v$) with depth recorded soon after every blow. Near the ground level, $\Delta u_{\max}/\sigma_v$ shows large value. However, it precipitously decreases and converges at some particular level. These changing points which converge into a zero have similarities with the groundwater table (shown in Figure 7 with groundwater table mark) acquired in boring exploration. Figure 8 shows correlation between the groundwater tables acquired in boring exploration and in evaluation by the *DPTU*. The result of our evaluation clearly shows that the correlations are substantially correspondent.

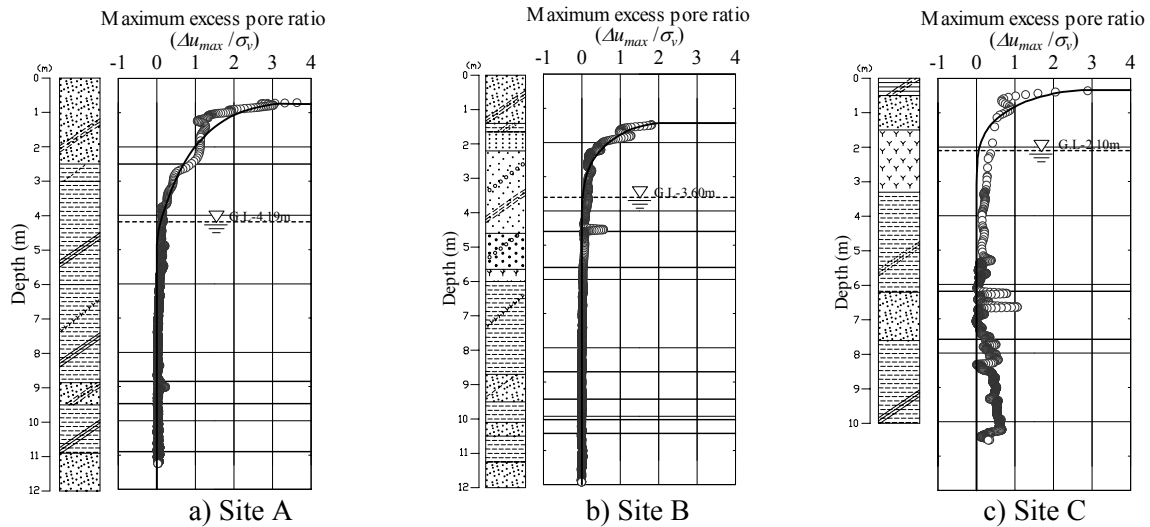


Figure 7. Depth distribution examples of maximum excess pore pressure ratio

Evaluation of soil type distribution (fine fraction content: F_C).

The excess pore pressure dissipation during dynamic penetration depends on the coefficient of permeability (k). In high fine fraction content soil, we can get bigger residual cumulative pore pressure (u_R) than in less fine-grained soil. Figure 9 shows the relationship between residual cumulative pore pressure ratio (u_R/σ_v) and fine fraction content (F_C) which previously obtained from the laboratory test using disturbed sample by *SPT*.

Correlation between u_R/σ_v and F_C correlation was led formula (2).

$$F_C = 18 \cdot (u_R / \sigma_v) \quad (0 \leq u_R / \sigma_v < 5.56) \quad (2)$$

$$\text{When } F_C = 100 \quad (u_R / \sigma_v \geq 5.56)$$

The figure 10 graphically shows one example of soil type distribution led by formula (2).

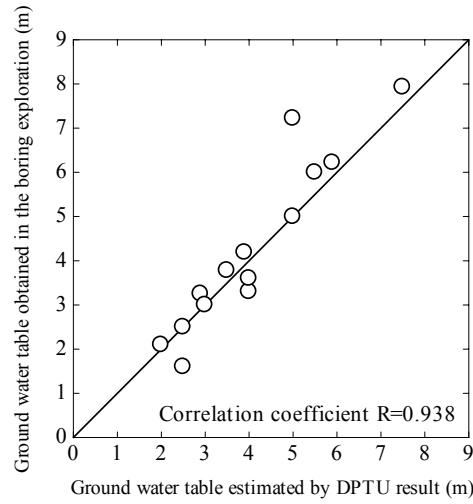


Figure 8. Measurements and estimate of groundwater table

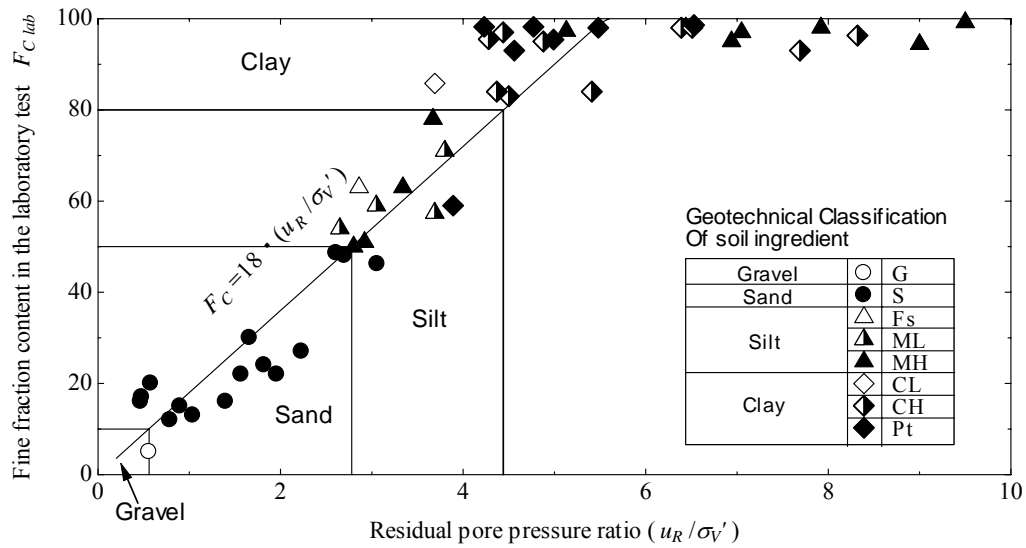


Figure 9. Relationship between residual cumulative pore pressure and fine fraction content F_C

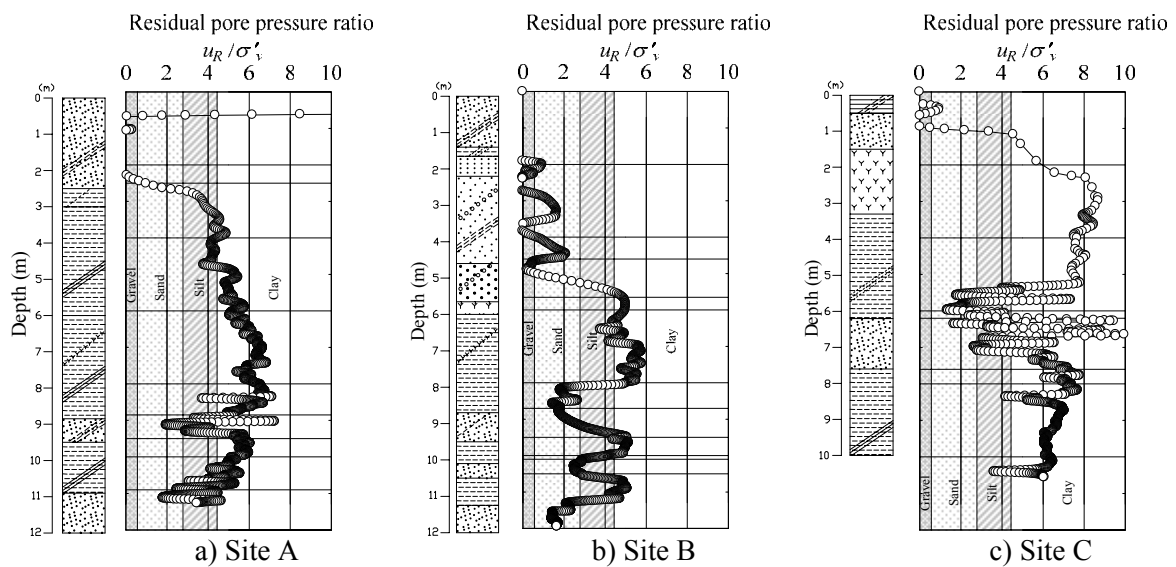


Figure 10. Depth distribution of residual pore pressure ratio

Evaluating liquefaction resistance

Flow chart for data processing to estimate liquefaction susceptibility by *DPTU* is shown in Figure 11. Maximum excess pore pressures (Δu_{\max}), Residual cumulative pore pressure (u_R), Penetration displacement and the depth of investigation without unit weight (γ_i) are able to be obtained by *DPTU*. As the flow indicates, γ_i is necessary to evaluate total overburden pressure (σ_v). Estimation procedure begins by calculating σ_v using depth of investigation and assumed γ_i in first step. Secondly, we can evaluate the groundwater table by maximum excess pore pressure ratio ($\Delta u_{\max}/\sigma_v$). Next, effective overburden pressure (σ'_v) is calculated using the groundwater table (*GWT*). And, we can evaluate the residual cumulative pore pressure ratio (u_R/σ'_v), then estimate the soil property classification and fine fraction content (F_c). By resetting γ_i by the soil classification or F_c , we can recalculate σ_v and σ'_v and re-estimate *GWT* with $\Delta u_{\max}/\sigma_v$ and F_c with u_R/σ'_v . When this re-evaluated γ_i substantially coincide with the estimate value, iteration will be closed. This iteration generally converges with once or twice, because it is not sensitive to γ_i . On the other hand, N_d value can be derived from the blow penetration and correspond to N_{SPT} value. As far as γ_i , *GWT*, F_c , N value are clear, we can estimate liquefaction susceptibility which is indicated in design specifications. The distribution of the liquefaction resistance with depth is shown in Figure 12. This figure indicates the comparison between the evaluations of liquefaction resistance (R_{DPTU}) by *DPTU* and liquefaction resistance (R_{SPT}) by *SPT* N value and the result of the data in a laboratory tests using disturbed samples.

It also indicates the average of liquefaction resistance amount in the *SPT* investigation section. In the liquefaction susceptibility appraisal, liquefaction resistance factor (F_L) was calculated by the seismic design specifications for Japanese Highway Bridges. The distribution of F_L with depth is shown in Figure 13. In this figure, the results of F_L are condition of Level 2 earthquake and Type-I which is the inter-plate type earthquake. One significant progress is that this new investigation method enables it to gather more accurate liquefaction susceptibility which we could not evaluate in conventional *SPT* appraisal and results of laboratory tests. The correlation of liquefaction resistance factor F_L value estimated in usual *SPT* and average F_L value of each *SPT* section in *DPTU* is shown in Figure 14. Though there are insufficient data and still need to be improved, generally both values positively correlate with each other.

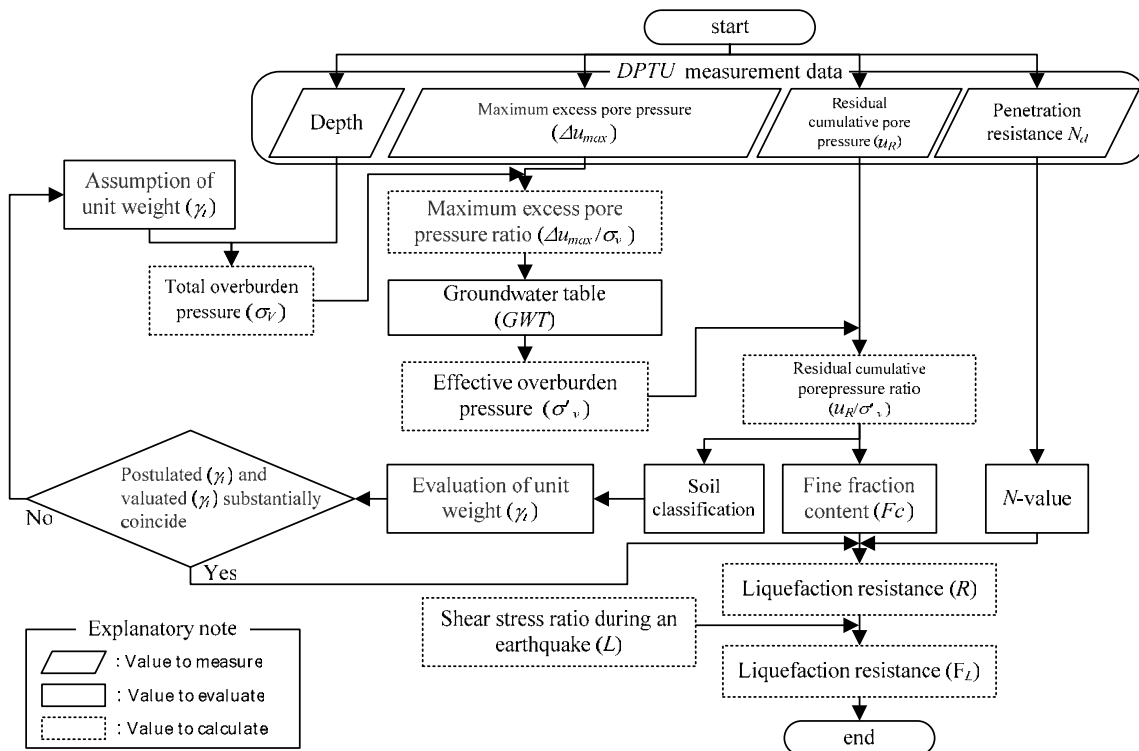


Figure 11. Evaluation flow of liquefaction potential

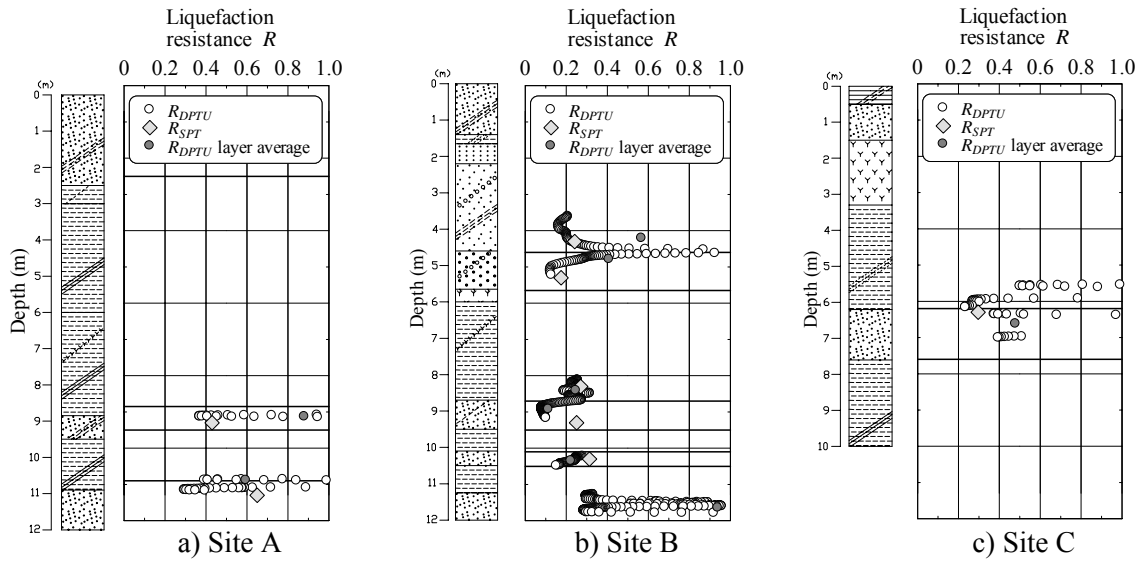


Figure 12. Depth distribution of liquefaction resistance

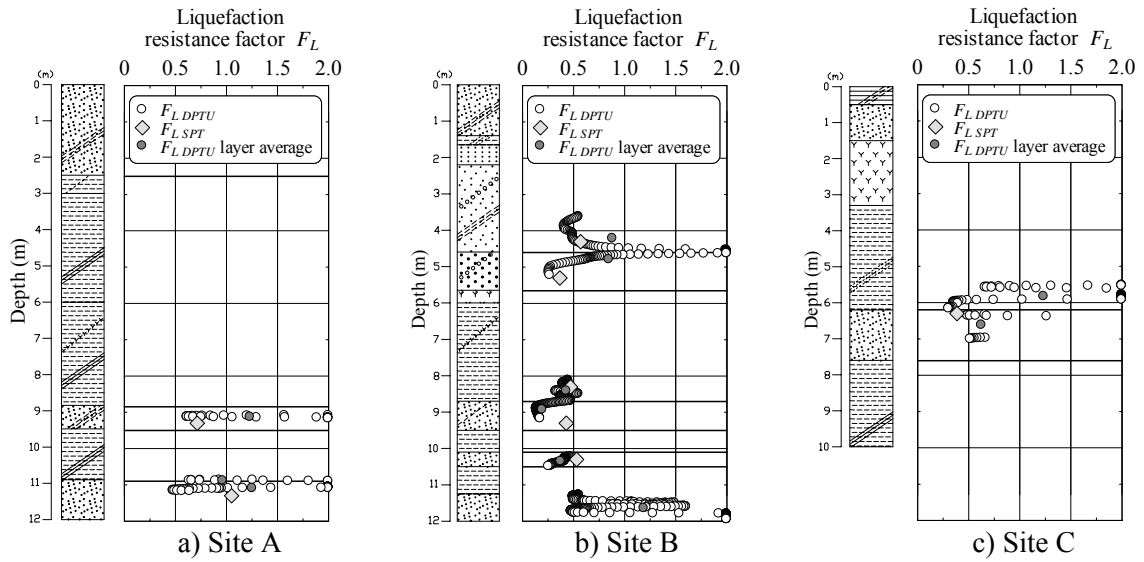


Figure 13. Depth distribution of liquefaction resistance factor

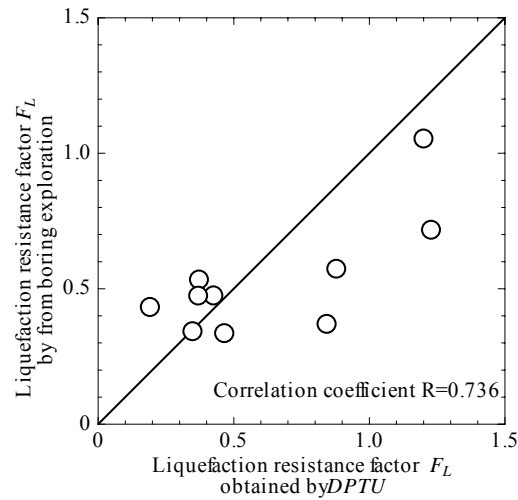


Figure 14. Depth distribution of liquefaction resistance factor

CONCLUDING REMARKS

The following conclusions were obtained from a series of dynamic penetration test results with pore pressure transducer which is named “*Piezo Drive Cone*”.

- (a) The distributions of the converted N_d value by a single blow can be used to identify the uniformity of layer and to find inter-bedded thin layers.
- (b) The time histories of pore pressure responses during dynamic penetration are significantly affected by the groundwater table
- (c) The residual cumulative pore pressure responses at the end of the penetration phase after blow indicate the classification and identification of soils which contains the fine fraction content (F_C).
- (d) The flow is proposed to estimate liquefaction susceptibility.

The significant progress is that this new investigation method enables it to gather more accurate liquefaction susceptibility which we could not evaluate in conventional investigation method such as *SPT* and the result of laboratory tests using samples. In the future direction of this study, we will develop more economic and simple in-situ apparatus for estimating the liquefaction susceptibility of soils.

REFERENCES

- 1) Sawada, S. “Estimation of liquefaction potential using dynamic penetration with pore pressure transducer,” International Conference on Cyclic Behavior of Soils and Liquefaction Phenomena, Bochum, pp. 305-312, 2004
- 2) Sawada, S., Tsukamoto, Y. & Ishihara, K. “Method of dynamic penetration with pore pressure transducer. Part 1 Test equipment and procedures,” Proc. Japan National Conference on Geotechnical Engineering, 39, pp.1927-1928, 2004 (in Japanese)
- 3) Sawada, S., Tsukamoto, Y. & Ishihara, K. “Method of dynamic penetration with pore pressure transducer Part 2 Results of chamber test,” Proc. JSCE Annual Conference, 59, pp.815-816, 2004 (in Japanese)
- 4) Sawada, S., Tsukamoto, Y. & Ishihara, K. “Method of dynamic penetration with pore pressure transducer. Part 3 Results of In-situ Test,” Proc. Geotechnical engineering symposium, 49, pp.15-20, 2004 (in Japanese)
- 5) Sawada, S., Tsukamoto, Y. & Ishihara, K. “Method of dynamic penetration with pore pressure transducer. Part 4 Soil classification system,” Proc. Japan National Conference on Geotechnical Engineering, 40, pp.1120-1121, 2005 (in Japanese)
- 6) Sawada, S., Tsukamoto, Y. & Ishihara, K. “Method of dynamic penetration with pore pressure transducer Part 5 The ground water level,” Proc. JSCE Annual Conference, 60, pp.961-962, 2005 (in Japanese)
- 7) Sawada, S., Tsukamoto, Y. & Ishihara, K. “Method of dynamic penetration with pore pressure transducer. Part 6 Liquefaction resistance,” Proc. Geotechnical engineering symposium, 50, pp.1-6, 2005 (in Japanese)
- 8) Japan Road Association “Seismic Design Specifications for Highway Bridges,” pp.120-126, 2002 (in Japanese)
- 9) Architectural Institute of Japan “Recommendations for Design of Building foundations,” pp.61-72, 2001 (in Japanese)
- 10) Port and Harbour Association, “Technical Standards and Commentaries for Port and Harbour facilities in Japan,” pp.281-288, 1999 (in Japanese)
- 11) Railway Technical Research Institute, “Seismic Design for Railway Structures,” pp.54-59, 1999 (in Japanese)
- 12) Ito, Y., Ogawa, S., Iwasaki, T., Murata, Y. and Sato, M. “Evaluation of ground condition using the light weight automatic ram sound,” Proc. Japan National Conference on Geotechnical Engineering, 37, pp.103-104, 2002 (in Japanese)